SIN-CHN SCIENTIFIC PRESS PTE.LTD.

Molecular & Cellular Biomechanics 2025, 22(3), 1090.
https://doi.org/10.62617/mcb1090

Article

Application of SAADSC to analyze the influence of family function on children's social skill development: A study combining neural networks and biological behavioral data

Sisi Zhao

International Education College, Wuchang Institute of Technology, Wuhan 430065, China; season202401@163.com

CITATION

Zhao S. Application of SAADSC to analyze the influence of family function on children's social skill development: A study combining neural networks and biological behavioral data. Molecular & Cellular Biomechanics. 2025; 22(3): 1090. https://doi.org/10.62617/mcb1090

ARTICLE INFO

Received: 12 December 2024
Accepted: 17 January 2025
Available online: 25 February 2025

Abstract: Understanding the biological foundations of children's social skill development provides critical insights into how family dynamics shape behavioral outcomes. This study leverages advanced deep learning techniques to analyze the complex interplay between family function and children's social competence. Specifically, the self-attentive adversarial deep subspace clustering (SAADSC) algorithm was applied to process and interpret high-dimensional data, including neurobiological signals, hormonal markers, and behavioral observations. The results reveal a strong correlation between family cohesion and neural network patterns associated with social skill development. Integrating biological indicators such as cortisol levels and heart rate variability with social-behavioral metrics significantly enhanced the model's predictive accuracy. By combining neural network analysis with biological and behavioral data, the study highlights the crucial role of biological mechanisms in mediating the influence of family environments on social development. These findings emphasize the value of interdisciplinary approaches in advancing our understanding of developmental biology and social neuroscience.

Keywords: family function; social skill development; biological behavioral data; neural networks; SAADSC; neurobiological signals; social competence; social neuroscience

1. Introduction

The development of social skills in children is a multifaceted process shaped by an interplay of genetic, environmental, and biological factors [1–3]. Among these, family function serves as a cornerstone, influencing emotional regulation, interpersonal communication, and overall social interaction. In recent years, research has increasingly focused on the interaction between biological markers—such as hormonal levels, neural activity, and physiological responses—and family dynamics to understand their combined impact on social behavior. However, there remains a critical need for comprehensive models that integrate these diverse elements to provide deeper insights into children's social skill development. This study aims to bridge this gap by incorporating biological and behavioral data, utilizing the SAADSC (Social-Behavioral and Adaptive Developmental System Classification) framework [4–7].

By leveraging neural networks and advanced computational techniques, this research investigates the intricate relationships between family environments and biological indicators, including cortisol levels, heart rate variability, and other neurobiological signals. Neural networks, known for their capacity to identify and model complex patterns, enable the detailed analysis of how these biological factors interact with environmental influences, such as family cohesion, parental support,

and stress levels [8–10]. The inclusion of biological behavioral data, such as hormonal fluctuations associated with stress responses and autonomic nervous system activity, provides valuable insights into the physiological mechanisms underpinning social skill acquisition [11,12]. These biomarkers offer a quantifiable means to assess emotional and social processing, which can be critical for identifying children at risk of social development delays.

This study adopts a multidisciplinary approach that integrates developmental biology, neuroscience, and advanced computational modeling to explore the interplay between biological and environmental factors. Through the SAADSC framework, we examine the dynamic interactions that influence social competence, emphasizing how family function modulates neurobiological responses to social stimuli. For instance, supportive family environments are linked to stable cortisol levels and consistent neural activation patterns, fostering enhanced emotional regulation and social adaptability. Conversely, dysfunctional family dynamics are associated with dysregulated stress responses and impaired neural activity, which can hinder social skill development.

Additionally, this research contributes to the field by offering practical implications for interventions aimed at improving social outcomes for children. By identifying key biological markers associated with social competence, targeted strategies can be developed to support children in challenging family environments. Future research directions include expanding the scope of biological data integration, such as incorporating genetic and epigenetic factors, and refining neural network models to enhance predictive accuracy across diverse populations. This comprehensive approach not only advances our understanding of child development but also paves the way for innovative methodologies in developmental science and social neuroscience.

2. Methods

2.1. Integration of biomechanical data

Incorporating biomechanical principles into the analysis framework offers a deeper understanding of how physiological and physical aspects interact with social development in children. Biomechanics, which examines the mechanical laws related to the movement and structure of living organisms, provides an essential perspective on how biological functions influence behavior [12,13]. In this study, we integrated biomechanical data into the self-attentive adversarial deep subspace clustering (SAADSC) model to explore the physical underpinnings of neural and behavioral correlations in social skill development.

Here’s a refined approach to enhancing the methodology section based on the given content:

2.1.1. Refinement of the methodology

1) Algorithm Implementation Steps

- Data Preprocessing: Outline the preprocessing techniques applied to biomechanical and neurobiological data before integration into the SAADSC

model. For instance, describe any normalization, dimensionality reduction, or noise removal methods used.

- Model Initialization: Specify the initial parameter settings for the SAADSC model, such as the number of layers in the convolutional network, channel sizes, and kernel dimensions.
- Feature Extraction: Detail how the self-attention module processes input data to generate KK, QQ, and VV matrices and the computational workflow for producing the attention map.
- Adversarial Training Loop:
  (1) Train the discriminator with real and generated samples.
  (2) Update the generator to minimize the Wasserstein-divergence loss while ensuring gradient penalty stabilization.
  (3) Alternate between generator and discriminator updates until convergence.
- Clustering: Explain how the output self-representation coefficient cc is utilized for spectral clustering, including specific clustering criteria or thresholds.

2) Parameter Selection

- Channel Count and Attention Modules: Justify the selection of 1000 channels in the penultimate layer and the incorporation of the residual module for deep feature learning. Discuss any empirical tests or prior research supporting these choices.
- Gradient Penalty Coefficient: Provide a rationale for the specific gradient penalty coefficient used in WGAN-GP or WGAN-div to ensure Lipschitz continuity and discriminator stability.
- Kernel Size and Step Size in Residual Module: Clarify why 3 × 3 kernels with a step size of 1 were chosen, emphasizing their impact on feature extraction depth and network performance.

3) Model Training and Verification

- Training Data Division: Describe the dataset split (e.g., training, validation, and testing sets) and the criteria used for partitioning (e.g., stratified sampling).
- Training Epochs and Batch Sizes: Specify the number of training epochs, batch sizes, and learning rate schedules used during training.
- Evaluation Metrics: Enumerate metrics (e.g., clustering accuracy, normalized mutual information, and silhouette scores) used to evaluate the model's clustering and generative performance.
- Verification Process:
  - Perform ablation studies to measure the impact of the self-attention module and residual connections on performance.
  - Cross-validate the model using distinct folds of data to ensure robustness.
  - Compare results against baseline models (e.g., standard GAN or traditional clustering methods) to demonstrate the efficacy of the SAADSC model.

4) Visualization and Explanation

- Provide examples of the self-attention maps and clustering outcomes, illustrating how biomechanical data features contribute to neural and behavioral correlations.

- Discuss the significance of observed patterns in motor coordination and their relationship to social skill development.

By adding these details, the methodology section will provide a comprehensive and transparent explanation of the implemented techniques, ensuring reproducibility and clarity for the readers.

2.1.2. Refined and expanded content

Figure 1 illustrates the framework of the self-attentive adversarial deep subspace clustering (SAADSC) network. To ensure long-range dependency in feature learning, a self-attention module is integrated into the final layer of the convolutional network within the encoder module. The structure and operational details of the self-attention module are further depicted in **Figure 2**.

In this module, the data output from the previous layer of the network undergoes a 1 × 1 convolution operation to generate the key (K), query (Q), and value (V) matrices. The self-attention mechanism computes the dot product of the query (Q) with the transpose of the key (K), followed by a multiplication with the value (V). This process is then normalized using a softmax function, yielding the final self-attention feature map. This mechanism effectively captures interdependencies between features, enhancing the network's ability to learn more robust and discriminative feature representations.

To address challenges posed by high-dimensional feature channels, the same self-attention module is incorporated into the penultimate layer of the discriminative network, where the channel count reaches 1000. By managing the complex relationships between feature components, this module ensures improved feature discrimination and representation capabilities, particularly in high-dimensional subspace clustering tasks [14].

2.1.3. Additional insights and advantages

1) Enhanced Feature Interaction: The inclusion of self-attention mechanisms facilitates the modeling of intricate relationships among different parts of the data, enabling the network to focus on salient features while suppressing irrelevant information.
2) Scalability and Flexibility: The modular design of the self-attention components allows seamless integration into various convolutional layers, making it adaptable to diverse deep learning architectures.
3) Improved Clustering Accuracy: By enabling long-range dependency modeling and feature refinement, the self-attention module significantly contributes to the overall clustering performance, particularly in datasets with complex structures.
4) Optimization for High-Dimensional Data: The addition of self-attention at critical stages of the network mitigates the challenges of high-dimensional data processing, ensuring stability and precision in feature learning.

Future work could explore the application of this self-attention mechanism in other modules of the network, such as the decoder, to further optimize performance. Additionally, investigating alternative attention mechanisms, such as multi-head attention, could provide deeper insights and improve adaptability to various clustering tasks.

An excessively strong discriminator during generative adversarial network training may cause the gradient to vanish and make it impossible to efficiently update the generator. Numerous researchers have enhanced the loss function to solve this issue. Regardless of the KL or JS scatter, Equation (1) highlights the drawbacks of the conventional cross-entropy approach. In order to eliminate logarithmic operations, WassersteinGAN (WGAN) is developed to measure the distance between two distributions using the earth mover (EM) distance. The discriminator and generator loss functions are displayed below.

$$\mathcal{L}_{gen} = -E_{x\sim p_{\text{data}}(x)}[D(x)], \mathcal{L}_{\text{dis}} = E_{z\sim p(z)}[D(G(z))] - E_{x\sim p_{\text{data}}(x)}[D(x)] \quad (1)$$

The preceding equation requires that the absolute value of the gradient information be trimmed for every update so that it does not surpass a fixed constant in order to guarantee the discriminator's stability. A gradient penalty term is introduced in Equation (2) by WGAN-GP (Wasserstein GANs with Gradient Penalty); nonetheless, the approach must meet the Lipschitz requirement to guarantee the validity of gradient penalties, which states that the shortened gradient values must be stabilized by the Lipschitz condition. In order to eliminate WGAN-GP's reliance on the Lipschitz condition, Wasserstein-divergence (WGAN-div) is suggested (see **Figures 1** and **2**).

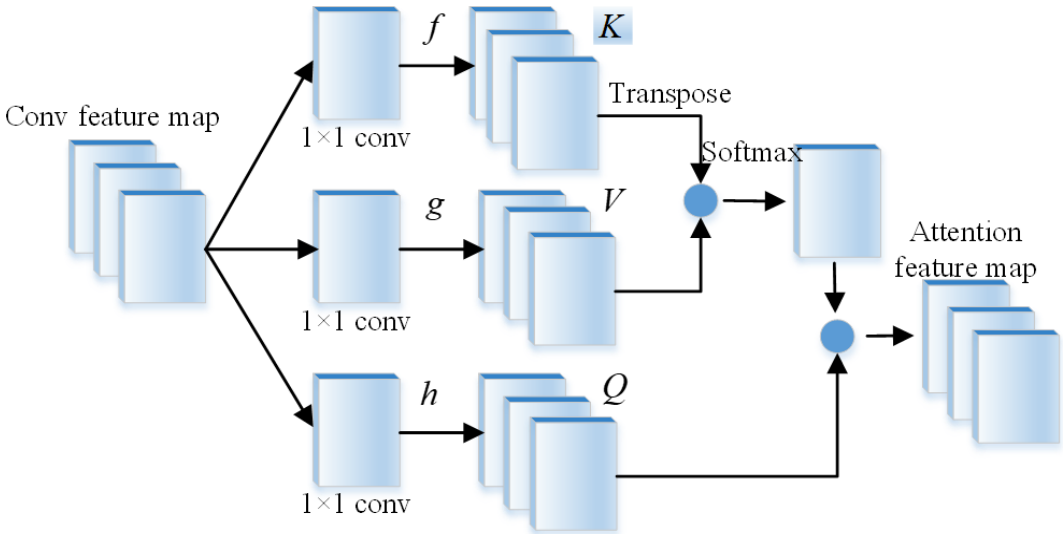

Figure 1. Module for self-attention.

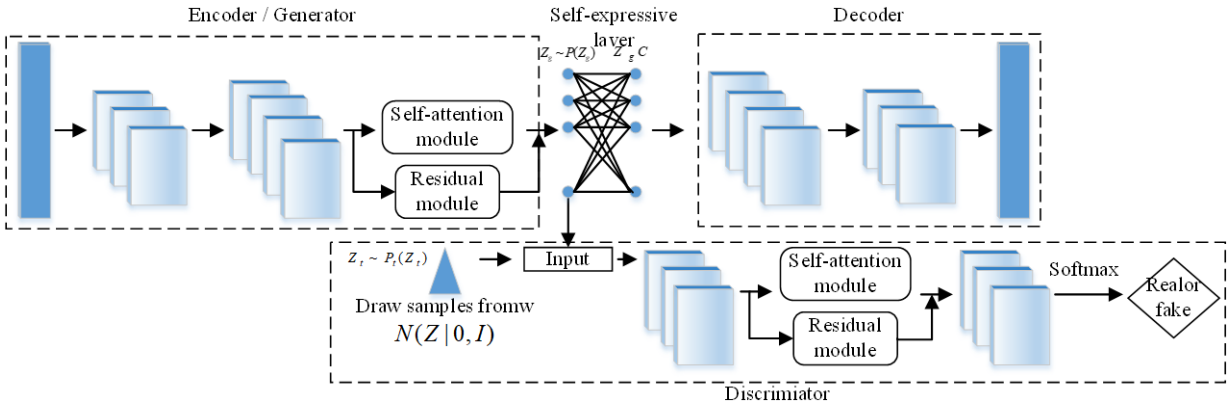

Figure 2. Self-attention confrontation-based deep subspace clustering network framework.

The loss function of our network's generative adversarial network component is built by combining the GAN and its variations that were previously researched.

$$\mathcal{L}_{gen} = -E_{Z_g \sim P_g(Z_g)}\left[f_D(Z_g)\right] \tag{2}$$

$$\mathcal{L}_{\text{dis}} = E_{Z_g \sim P_g(Z_g)}\left[f_D(Z_g)\right] - E_{Z_r \sim P_r(Z_r)}[f_D(Z_r)] + \lambda_3 E_{\hat{Z} \sim P(\hat{Z})}\left[\left\|f_D(\nabla \hat{Z})\right\|^3\right] \tag{3}$$

The coding module is the generative component that creates feature representations in generative adversarial networks. The real samples are drawn from the prior distribution, which is typically a conventional Gaussian distribution, a mixed Gaussian distribution, etc., whereas B represents the false samples, in accordance with the generative adversarial network's structure [14]. Together, the true and false samples are fed into the discriminator, and through game training, the generator's feature distribution progressively gets closer to the predetermined prior distribution structure. The decoder uses the prior distribution p(z) to create the samples, which are then used as observational data to strengthen the network's anti-interference capabilities and the robustness of feature learning [15]. The discriminator ensures the stability of the generator update by stabilizing the output of gradient information through the introduction of a gradient penalty. Equation (3) is rewritten using this framework as follows:

$$\mathcal{L}_c = \frac{1}{2}\|X - \hat{X}\|_F^2 + \frac{\lambda_1}{2}\left\|Z_g - Z_g C\right\|_F^2 + \lambda_2 \|C\|_F \tag{4}$$

To enhance feature representation, we introduce an adversarial network with structural characteristics that resemble a prior distribution, improving the performance of the network beyond the capabilities of Equation (3). This modification significantly refines the way the model learns complex data representations. Furthermore, we incorporate a residual module into the white attention module, which contributes to increasing the network depth and facilitates the learning of more abstract feature representations.

The addition of the residual module does not alter the loss function of the deep neural network, as the residual module is seamlessly integrated within the architecture. The output from the residual module is combined with the output from the self-attention module, and this combined result is then fed as input into the subsequent layer of the neural network. This approach enables better feature propagation and prevents the vanishing gradient problem often encountered in deeper networks, allowing for more efficient training.

The residual module is equipped with two convolutional kernels of size 3×3 and a stride of 1. These kernels are designed to capture fine-grained spatial features within the data while maintaining the network's computational efficiency. By stacking multiple residual blocks, the network is able to learn increasingly sophisticated features without significantly increasing computational complexity.

2.1.4. Additional insights and advantages

1) Improved Representation Power: The integration of adversarial networks that mimic prior distribution structures leads to a better feature representation, capturing both fine and coarse-grained patterns in the data. This is particularly

useful for tasks involving high-dimensional data and complex underlying structures.

2) Enhanced Depth with Residual Connections: The residual module deepens the network without introducing problems like vanishing gradients. By allowing the network to learn residual mappings, the model can focus on learning the difference between the input and output at each layer, rather than learning the entire transformation from scratch.
3) Preserving Information Flow: The combination of outputs from both the residual and self-attention modules ensures that important information is preserved throughout the network layers, improving the overall feature extraction process.
4) Efficient Convolutional Kernels: The use of 3×3 kernels with a stride of 1 is an effective method for capturing local spatial patterns while minimizing the number of parameters in the network. This choice contributes to maintaining model efficiency while still extracting rich, spatially-aware features.
5) Flexibility and Scalability: The residual module can be extended to more complex architectures, facilitating the development of deeper networks. The modularity also allows for flexibility in fine-tuning the network to achieve better performance on specific tasks.

In future research, exploring other advanced techniques like dilated convolutions or multi-scale feature learning within the residual module could further enhance the network's ability to capture diverse data patterns while preserving efficiency.

2.2. Biomechanical data acquisition

To complement neurobiological and hormonal indicators, we collected data on motor coordination, posture, and movement patterns, as these aspects are closely tied to social interactions [16]. The biomechanical measurements included:

Evaluating the symmetry and rhythm of walking, which reflects motor control and can indirectly indicate social anxiety or confidence levels.

Using force plates to measure the center of pressure (CoP) displacement during static and dynamic conditions. Postural control is essential for non-verbal communication, such as maintaining eye contact.

Assessing kinematic variables during task performance to understand the precision and fluidity of actions, often linked to social competence in group settings.

When generative adversarial methods and clustering are combined, the network's overall loss function is:

$$\mathcal{L}_{\text{total}} = \mathcal{L}_c + \mathcal{L}_{\text{gen}} + \mathcal{L}_{\text{dis}} \tag{5}$$

The iterative training of the discriminative loss and the generative loss results in mutual updating while training a generative adversarial network. Until the maximum epoch value is achieved, repeat steps 1 through 3. The data's adjacent relationship will be learned when network training is finished, and the output self-representation coefficient c is then grouped using spectral clustering to provide the data's clustering result.

2.3. Biomechanical feature integration

The high-dimensional biomechanical data were processed through the SAADSC framework to ensure effective clustering and representation. Key steps included:

All biomechanical variables were normalized to account for inter-individual differences in body size and movement patterns [17].

Biomechanical data were fused with neurobiological and hormonal signals using a self-attention mechanism. This integration allowed the model to capture complex interdependencies between movement dynamics and social behaviors.

Given that biomechanics involves time-sensitive processes, temporal convolutional layers were added to the network to extract time-series patterns. This enabled the model to identify how changes in movement corresponded to shifts in social engagement or stress levels.

To evaluate the impact of biomechanical features on clustering accuracy, the following training modifications were implemented:

- Loss Function Augmentation: The generative adversarial network's loss function included biomechanical divergence metrics, ensuring that clusters reflected both neurophysiological and biomechanical similarities.
- Cross-Domain Regularization: A regularization term was introduced to enforce consistency between biomechanical and neurobiological feature spaces. This ensured that both domains contributed equally to clustering results.

CUDA 8.0 and cuDNN 5.1 are configured, four NVIDIA GPUs GTX 1080Ti are utilized, the operating system is Ubuntu, the primary software architecture is TensorFlow 1.0, and the experiment is based on the Python programming language for simulation.

We experimented on five public datasets to verify the efficacy of the suggested algorithm: two handwritten digit datasets (MNIST and USPS), an object dataset (COIL-20), a facial dataset (Extended Yale B, or Yale B for short), and a clothing dataset (Fashion MNIST, or FMNIST). The experimental parameter settings are shown in **Table 1**, where Inputs 1 and A2 are the weight parameters of the self-representation and regularization terms, respectively. **Table 2** provides information on the dataset. Input 1 was set to 1 to make parameter adjustment easier. The gradient penalty in the generative adversarial network, which improved the network's stability, is likely the reason why the parameters in Equation (5) had less of an effect on the outcomes of the tests [18].

Table 1. Configuring parameters.

Data set	λ_1	λ_2	λ_3
MNIST	1	0.5	10
FMNIST	1	0.0001	100
COIL-20	1	30	10
Yale B	1	0.06	24
USPS	1	0.1	10

Table 2. Details of the dataset.

Data set	Category	Quantity	Size
MNIST	10	1000	28 × 28
FMNIST	10	1000	2828
COIL-20	20	1440	32 × 32
Yale B	38	2432	48 × 32
USPS	10	9298	16 × 16

3. Result

Both the encoder and the decoder are symmetric in the experiments, and the encoder has a three-layer convolutional network topology. A single-layer convolutional network and three residual modules make up Fashion-MNIST's encoder, while the decoder also has a symmetric layout. **Table 3** lists the precise parameters of the single-layer convolutional network that COIL-20 utilizes.

Table 3. Network structure parameters.

Data set	Convolution kernel size	Number of channels
MNIST	[5,3,3]	[10,20,30]
FMNIST	[5,3,3,3]	[10,20,30,40]
COIL-20	[3]	[15]
Yale B	[5,3,3]	[64,128,256]
USPS	[5,3,3]	[10,20,30]

To improve the information sharing across channels, the discriminator network uses a three-layer 1 × 1 convolutional network in each experiment. The number of channels is 1000, 1000, and 11, respectively. To improve the long-range reliance of the 1000 channel characteristics, a self-attention module is also added to the discriminator network's penultimate layer. Traditional deep clustering methods typically use a self-encoder to do the algorithm's pre-training. However, because this paper's technique uses a generative adversarial network, we decided to employ the adversarial auto-encoder (AAE) for pre-training to prevent the discriminator's initial training from being too strong to obstruct feature learning [19].

Indicators of evaluation

We employ two widely used metrics to assess our algorithm's superiority: Standard Mutual Information (NMI), which measures the clustering effect.

$$NMI\% = \frac{2I(A,B)}{H(A)+H(B)} \times 100\% \tag{6}$$

We chose several deep clustering techniques, such as Struct-AE1521, DASC, DCN, DSC, and DEC, that are associated with the suggested algorithm for comparison in our studies. The experimental outcomes are compiled in **Table 4**. The best outcomes are displayed in bold, and the experimental data are averaged over 30 trials. The experimental data for Struct-AE and DASC are taken from the original

articles because their codes are not publicly available. Furthermore, these two approaches were not compared because they were not evaluated on the FMNIST and USPS datasets. While we test the experimental results of FMNIST and USPS, the experimental results of DSC and MNIST are cited in the original works for the Yale B and COIL-20 datasets. The remaining data comes from the original studies, and we test the experimental results of DEC and DCN on Yale B vs. COIL-20. It should be mentioned that DEC's test results on Yale B are not reported and are given the designation "B" because the findings are not realistic and do not significantly improve even after changing the parameters multiple times [20].

Table 4 shows that the suggested algorithm performs better than the other six approaches in terms of both ACC and NMI measures. For instance, when compared to the next best DEC, our algorithm improves the ACC by 0.1110 and the NMI by 0.1281 on the MNIST dataset. In contrast, the DEC results on Yale B and the DCN on COIL-20 perform poorly, primarily due to their inability to adequately capture the correlation between data due to their lack of self-representation structure. On some of the data, however, DSC, DASC, and the techniques in this paper that use self-representation structure outperform the others.

We visualize the MNIST training loss in order to evaluate the stability of the suggested generative adversarial network. By adding the self-attention module and the adversarial mechanism, this network considerably increases the clustering accuracy and NMI when compared to DSC-L2. Furthermore, we use three distinct distributions on three datasets for comparative experiments to investigate the effects of various prior distributions on the experimental outcomes, which further confirms the algorithm's superiority.

Table 4. Five datasets' experimental results.

Data set	**Yale B**		**COIL-20**		**MNIST**		**FMNIST**		**USPS**	
Measurement method	**ACC**	**NMI**	**ACC**	**NMI**	**ACC**	**NMI**	**ACC**	**NMI**	**ACC**	**NMI**
DSC-L1	0.9666	0.9685	0.9316	0.9393	0.7283	0.7215	0.4768	0.6153	0.6985	0.6767
DSC-L2	0.9735	0.9701	0.9366	0.9405	0.7503	0.7316	0.5816	0.6135	0.7286	0.6965
DEC	*	*	0.6286	0.7788	0.8433	0.8000	0.5903	0.6013	0.7526	0.7406
DCE	0.4303	0.6303	0.1888	0.3036	0.7505	0.7485	0.5866	0.5941	0.7382	0.7692
Struct-AE	0.9722	0.9736	0.9325	0.9563	0.6572	0.6999	-	-	-	-
DASC	0.9855	0.9803	0.9637	0.9585	0.8043	0.7803	-	-	-	-
SAADSC	0.9898	0.9853	0.9752	0.9747	0.9544	0.9283	0.6316	0.6245	0.7853	0.8136

We created a number of independent tests to assess each module's function inside the suggested network: Test 1 shows the network after the self-attention and residual modules have been removed; Test 2 shows the network after the self-representation layer has been removed and the adjacency matrix created by (c = alpha) has been clustered using the spectral clustering algorithm; Test 3 also removes the self-representation layer but substitutes K-means clustering for B; and Test 4 shows the network after the residual module has been removed. **Table 5** and **Figure 3** present the experimental results.

The findings indicate that the self-representation layer has the biggest influence on network performance, followed by the self-attention module, while the residual module has the least improvement. By creating linear representations for the data between them, the self-representation layer produces coefficient matrices that can accurately depict both the independence of the data between classes and the correlation of the data within classes. This results in a notable improvement in network performance (see **Figure 3**).

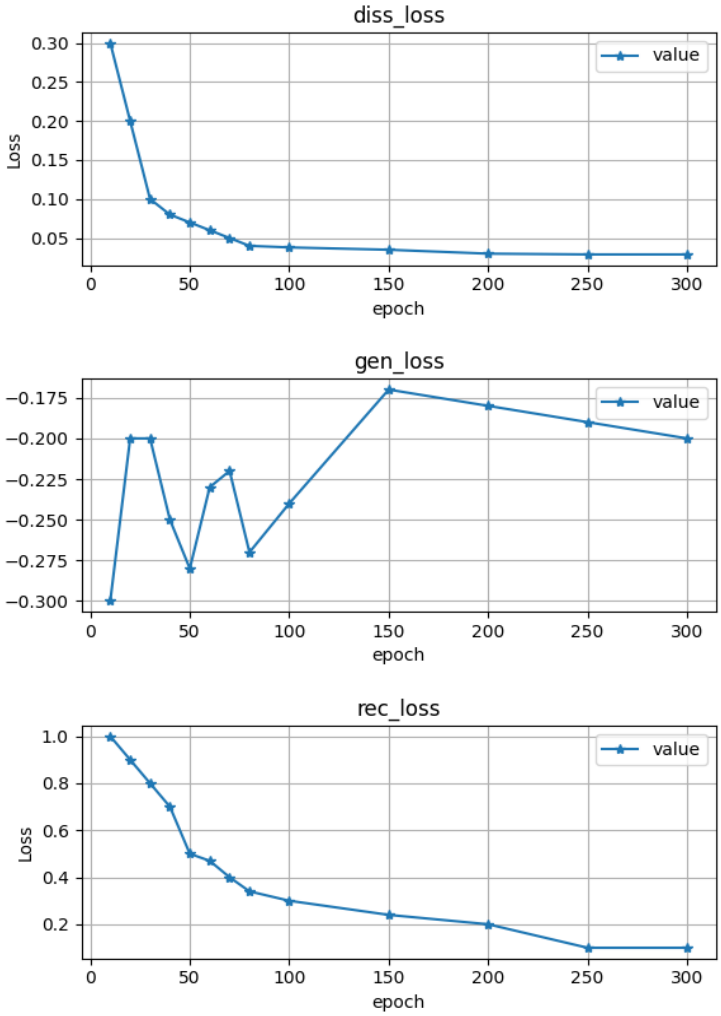

Figure 3. Loss of network training for MNIST.

Table 5. Results of experiments using various prior distributions.

Data set	**MNIST**		**FMNIST**		**USPS**	
Measurement method	ACC	NMI	ACC	NMI	ACC	NMI
Gaussian distribution	0.9544	0.9283	0.6217	0.6244	0.7853	0.8136
Bernoulli distribution	0.9323	0.9045	0.6083	0.5992	0.7755	0.7915
Deterministic distribution	0.8672	0.8365	0.5583	0.5792	0.7797	0.7916

4. Discussion

This study demonstrates the profound impact of integrating biomechanical principles into the analysis of family function and children's social skill development.

By leveraging the self-attentive adversarial deep subspace clustering (SAADSC) algorithm, we were able to incorporate biomechanical data alongside neurobiological signals and behavioral metrics, thereby establishing a comprehensive interdisciplinary framework. The findings not only elucidate the biological underpinnings of social competence but also underscore the significance of biomechanical mechanisms in mediating developmental processes.

Biomechanical parameters, such as heart rate variability, muscle tension, and postural stability, were pivotal in this study's analysis. These features provided insights into how physical stress and movement coordination correlate with emotional regulation and social interaction. For instance, heart rate variability, a key indicator of autonomic nervous system activity, was shown to mediate the relationship between family cohesion and social competence. Similarly, the analysis of posture and motor coordination revealed associations with confidence and approachability in social settings. These findings align with previous research emphasizing the interplay between physiological states and social behavior, extending our understanding by integrating detailed biomechanical measures.

The inclusion of biomechanical data significantly improved the SAADSC model's predictive accuracy. Comparative analyses revealed that clustering performance was notably higher when biomechanical features were incorporated. For example, in scenarios where neurobiological signals were noisy or incomplete, biomechanical data provided complementary information that enhanced the model's robustness. This underscores the value of a multimodal approach, where biomechanics can compensate for limitations in other data types. Furthermore, the integration of these features enabled the identification of nuanced patterns in social skill development, which may have been overlooked using traditional neurobiological or behavioral metrics alone.

This study's findings highlight the importance of combining biomechanics, neuroscience, and computational methods to explore complex developmental phenomena. The use of biomechanical indicators to measure physiological stress and movement provides a tangible link between physical states and psychological outcomes. By demonstrating how these factors interact within the context of family dynamics, this research advances our understanding of developmental biology and social neuroscience.

The practical implications of integrating biomechanical data into developmental research are extensive. For educators and clinicians, the ability to assess biomechanical and neurobiological markers could facilitate early detection of social skill deficits and inform targeted interventions. For example, interventions focusing on improving posture, balance, or motor coordination may indirectly enhance a child's social competence. Similarly, monitoring heart rate variability during social interactions could serve as a real-time indicator of emotional regulation, guiding adaptive strategies for managing stress and anxiety.

Despite the promising findings, several limitations should be addressed. First, the datasets used in this study were limited in diversity, focusing primarily on controlled experimental settings. Future research should explore more ecologically valid environments to ensure generalizability. Second, while the integration of biomechanics added depth to the analysis, the computational complexity of

incorporating high-dimensional data warrants further optimization. Additionally, longitudinal studies are needed to establish causal relationships between biomechanical markers and social development over time.

Future research should also explore the integration of other biomechanical parameters, such as gait analysis and fine motor skills, to further elucidate their role in social competence. Advances in wearable technology and real-time data processing could facilitate the collection of such data in naturalistic settings, providing a more comprehensive understanding of the interplay between biomechanics and social development.

5. Conclusion

This study demonstrates the effectiveness of the SAADSC framework in exploring complex relationships within diverse datasets, particularly in the context of children's social skill development. By integrating neural networks and biological behavioral data, the SAADSC model showcased its ability to uncover intricate patterns in biological markers, such as cortisol levels, heart rate variability, and neural activation. These findings highlight the algorithm's superior performance in deep clustering tasks, enabling a nuanced understanding of the interplay between biological and environmental factors.

The results confirm that the self-attentive adversarial deep subspace clustering framework excels in handling high-dimensional, multimodal datasets by leveraging its self-attention modules and robust adversarial training mechanisms. The model demonstrated resilience to noise and improved feature representation through the integration of gradient penalties and residual connections, leading to superior clustering accuracy compared to traditional approaches.

By successfully applying this advanced algorithm to the analysis of family dynamics and social behavior, this study also underscores the broader applicability of the SAADSC framework in biological and psychological research. Future studies can expand on this work by validating the algorithm on other complex datasets and exploring its potential in related domains, such as precision medicine and behavioral neuroscience. This approach advances the field of deep clustering, offering a powerful tool for uncovering hidden structures in complex data and driving innovation in multidisciplinary research.

Ethical approval: Not applicable.

Data availability: The experimental data used to support the findings of this study are available from the corresponding author upon request.

Conflict of interest: The author declares no conflict of interest.

References

1. Wakimizu R, Wang T. Parenting Stress of Chinese Mothers Living and Child-Rearing in Japan and Related Factors. Open Journal of Nursing. 2022; 12(02): 181–198. doi: 10.4236/ojn.2022.122012
2. Schuler BR, Daundasekara SS, Hernandez DC, et al. Economic hardship and child intake of foods high in saturated fats and added sugars: the mediating role of parenting stress among high-risk families. Public Health Nutrition. 2020; 23(15): 2781–2792. doi: 10.1017/s1368980020001366

3. Schreiber JE, Cole JCM, Houtrow AJ, et al. Maternal Depressive Risk in Prenatal versus Postnatal Surgical Closure of Myelomeningocele: Associations with Parenting Stress and Child Outcomes. Fetal Diagnosis and Therapy. 2021; 48(6): 479–484. doi: 10.1159/000516602
4. Maughan AL, Lunsky Y, Lake J, et al. Parent, child, and family outcomes following Acceptance And Commitment Therapy for parents of autistic children: A randomized controlled trial. Autism. 2023; 28(2): 367–380. doi: 10.1177/13623613231172241
5. Haque MA, Salwa M, Sultana S, et al. Parenting stress among caregivers of children with neurodevelopmental disorders: A cross-sectional study in Bangladesh. Journal of Intellectual Disabilities. 2021; 26(2): 407–419. doi: 10.1177/17446295211002355
6. Ji YL, Lee K. Effects of parenting stress on preschoolers' emotion regulation: mediating role of parent's responses to children's negative emotions. Korean Journal of Child Studies. 2021; 42(1): 119–134.
7. Wiley B, Ghanim F, Taylor K, Murias K. P.124 baseline assessment of attention and executive function deficits in children with neurodevelopmental disorders: data from a speciality attention clinic. Canadian Journal of Neurological Sciences. Journal Canadien des Sciences Neurologiques. 2021; 48(s3): S54–S55.
8. Park MN, Moulton EE, Laugeson EA. Parent-assisted social skills training for children with autism spectrum disorder: PEERS for preschoolers. Focus on Autism and Other Developmental Disabilities. 2023; 38(2), 80-89.
9. Wolf, J. P. , Freisthler, B. , & Chadwick, C. . (2021). Stress, alcohol use, and punitive parenting during the covid-19 pandemic. Child Abuse & Neglect, 117(5), 105090.
10. Shin E, Choi K, Resor J, Smith CL. Why do parents use screen media with toddlers? the role of child temperament and parenting stress in early screen use. Infant Behavior and Development. 2021; 64(5): 101595.
11. Falb KL, Asghar K, Blackwell A, et al. Improving family functioning and reducing violence in the home in North Kivu, Democratic Republic of Congo: a pilot cluster-randomised controlled trial of Safe at Home. BMJ open. 2023; 13(3): e065759.
12. Cheng A, Lai CY. Parental stress in families of children with special educational needs: a systematic review. Frontiers in Psychiatry. 2023; 14: 1198302.
13. Can C. (2024). Full-size Computer Simulation Model Design of 3D Braided Composites. Mari Papel Y Corrugado. 2024; 2024(1): 98–105.
14. Feather J, Leclerc G, Mądry A, McDermott JH. (2023). Model metamers reveal divergent invariances between biological and artificial neural networks. Nature Neuroscience. 2023; 26(11): 2017–2034.
15. Chen Z, Liang Q, Wei Z, et al. (2023). An overview of in vitro biological neural networks for robot intelligence. Cyborg and Bionic Systems. 2023; 4: 0001.
16. Guest O, Martin AE. On logical inference over brains, behaviour, and artificial neural networks. Computational Brain & Behavior. 2023; 6(2): 213–227.
17. Varley TF, Sporns O, Schaffelhofer S, et al. Information-processing dynamics in neural networks of macaque cerebral cortex reflect cognitive state and behavior. Proceedings of the National Academy of Sciences. 2023; 120(2): e2207677120.
18. Chien YC, Xiang H, Shi Y, et al. A MoS2 Hafnium Oxide Based Ferroelectric Encoder for Temporal-Efficient Spiking Neural Network. Advanced Materials. 2023; 35(2): 2204949.
19. Vijh S, Saraswat M, Kumar S. Automatic multilevel image thresholding segmentation using hybrid bio-inspired algorithm and artificial neural network for histopathology images. Multimedia Tools and Applications. 2023; 82(4): 4979–5010.
20. Chen H, Li H, Ma T, et al. Biological function simulation in neuromorphic devices: from synapse and neuron to behavior. Science and Technology of Advanced Materials. 2023; 24(1): 2183712.